Available online at www.sciencedirect.com

ScienceDirect

Procedia Structural Integrity 2 (2016) 1481–1488

Structural Integrity Procedia

www.elsevier.com/locate/procedia

21st European Conference on Fracture, ECF21, 20-24 June 2016, Catania, Italy

Hydrogen-induced failure of TiNi based alloy with coarse-grained and ultrafine-grained structure

Baturin A.[a,c]*, Lotkov A.[a,b], Grishkov V.[a], Rodionov I.[a], Krukovskiy K.[a]

[a]*Institute of Strength Physics and Materials Science SB RAS, 2/4, pr. Akademicheskii, Tomsk, 634021, Russia*
[b]*National Research Tomsk State University, Lenin Avenue, 36, Tomsk,634050, Russia*
[c]*National Research Tomsk Polytechnic University, Lenin Avenue, 30, Tomsk, 634050, Russia*

Abstract

The objective of this work is to investigate the effect of hydrogen-induced fracture of TiNi-based alloy. In this report we performed the first studies comparing inelastic properties and fracture of the specimens of the binary alloy of TiNi wire under the action of hydrogen with coarse-grained (CG) and ultrafine-grained (UFG) microstructure. It is shown that hydrogen embrittlement (HE) occurs irrespective of the grain size in the studied specimens at approximately equal strain values. However, compared to the specimens with CG structure, those with UFG structure accumulate two to three times more hydrogen for the same hydrogenation time. It is found that hydrogen has a much smaller effect on the inelastic properties of specimens with UFG structure as compared to those with CG structure.

Keywords: NiTi wire, fracture, hydrogen embrittlement, ultrafine grain

1. Introduction

Due to the good corrosion resistance and high biocompatibility, the products made of titanium nickelide (TiNi) are successfully used as medical implants. In particular, the superelastic TiNi wire is used in manufacturing of bracket systems. However, it has been found that these devices are prone to brittle failure in oral cavity after several

* Corresponding author.
E-mail address: abat@ispms.tsc.ru

10.1016/j.prostr.2016.06.188

months Yokoyama et al. (2001). The studies have shown that this process occurs due to the hydrogen embrittlement (HE) effect Asaoka et al. (2002); Yokoyama et al. (2012). This phenomenon is manifested in reduction of the wire superelasticity properties when hydrogen concentration inside the material increases and then the brittle failure of the wire takes place. Hydrogen can be released from the physiological medium and then be absorbed by a product made of TiNi under the action of galvanic currents. At present three main hypotheses are discussed in the literature concerning the mechanism of the HE phenomenon in TiNi-based alloys: hydride embrittlement, stressed hydrogen-martensitic interaction and formation of vacancy porosity. However, none of them was supported by convincing proofs. In the recent work of Kireeva et al. (2015), it was found that HE is also observed at hydrogenation of $Ti_{49.4}Ni_{50.6}$ monocrystals. The HE phenomenon occurs first, due to the decomposition of the Ni-enriched initial alloy under the action of hydrogen with phase separation of $TiNi_3$, which is observed in normal conditions only at high temperatures, and second, due to the precipitation of TiH hydrides. The effect of certain factors determining the HE phenomenon in TiNi using TiNi polycrystals (hydrogen concentration Pelton et al. (1997), strain rate Gamaoun et al. (2014), ageing time at room temperature Gamaoun et al. (2014); Gamaoun et al. (2011), etc. is studied. Besides, attention was drawn A.A. Ilin et al. (1984) to the hydrogen absorption dependence on the alloy structural state, including phase state. However, up to the present time, there were no attempts to study the effect of the grain size in TiNi-based alloys on the HE phenomenon. The urgency of this problem is determined by the growing use of products made of TiNi with ultrafine-grained (UFG) structure in medical practice. In this paper, we performed the first studies comparing inelastic properties of the specimens made of the binary alloy of TiNi wire under the action of hydrogen with CG and UFG structures. The fracture regularities of CG hydrogenated specimens are studied.

2. Materials and Research Methods

The tests were performed using the specimens of 1 mm diameter wire made of $Ti_{49,1}Ni_{50,9}$ (atom per cent), produced by the "Industrial Centre MATEK-SMA". The initial state of the wire after drawing is the UFG structure with an average grain/subgrain size of 0.1 – 0.2 μm. The CG wire specimens were obtained by the initial wire annealing at 973K for 30 min. with subsequent cooling in water. This treatment was done to form homogenous solid solution state B2 parent phase.

The microstructure of the recrystallized specimens was studied by optical metallography (AXIOVERT 200 MAT) and scanning electron microscopy. The results presented here were obtained using a LEO EVO 50 (Zeiss, Germany) scanning electron microscope NANOTEKh Center for Collective Use of the Institute of Strength Physics and Materials Science of the Siberian of the Russian Academy of Sciences. The microstructure of UFG samples was studied by electron microscopy (JEM-2100). The temperatures of martensitic transformations were calculated by the analysis of temperature dependence of electrical resistivity in heating and cooling wire specimens. M_S and M_f, are the temperatures, when upon cooling martensite (B19`) formation starts and finishes, respectively, and A_S, A_f, are the temperatures, when upon heating austenite (B2) formation starts and finishes, respectively.

The specimens have been charged electrolytically with hydrogen in 0.9% NaCl physiological solution at the current density of 20 A/m^2, saturation time was 3 hours. A cylindrical platinum plate was used as an anode. Hydrogen concentration was measured using a hydrogen analyzer RHEN602 of LECO. The study of inelastic properties was performed using an inverted pendulum device. Inelastic properties were determined in the cyclic loading and unloading scheme of the specimens under isothermal (293K) conditions.

3. Experimental Results and Discussion

Consider the grain structure of the initial samples prior to hydrogenation, their structural and phase state and mechanical properties.

Figure 1 shows a typical microstructure of the $Ti_{49.1}Ni_{50.9}$ alloy initial wire after drawing. The image was taken in a longitudinal section of the wire. The average grain/subgrain size is 0.1-0.2 μm.

Figure 2 shows the microstructure and histogram of the grain size distribution for the recrystallized specimens of the $Ti_{49.1}Ni_{50.9}$-alloy. Grain shape is close to the equiaxed with an average size of 8 μm.

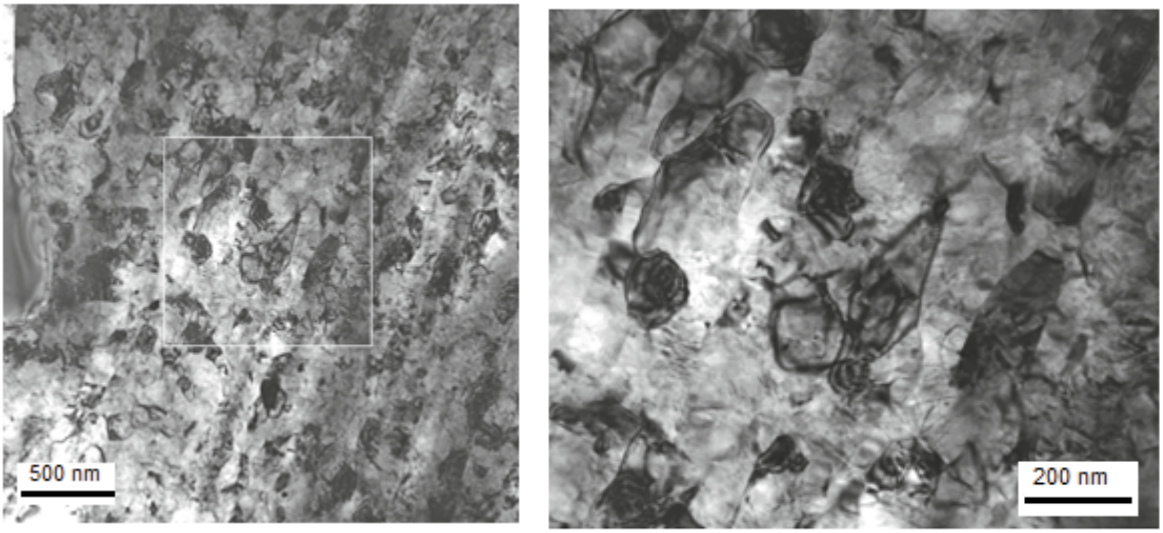

Fig. 1. Electron microscopic images of a typical microstructure of the UFG $Ti_{49.1}Ni_{50.9}$ specimens.

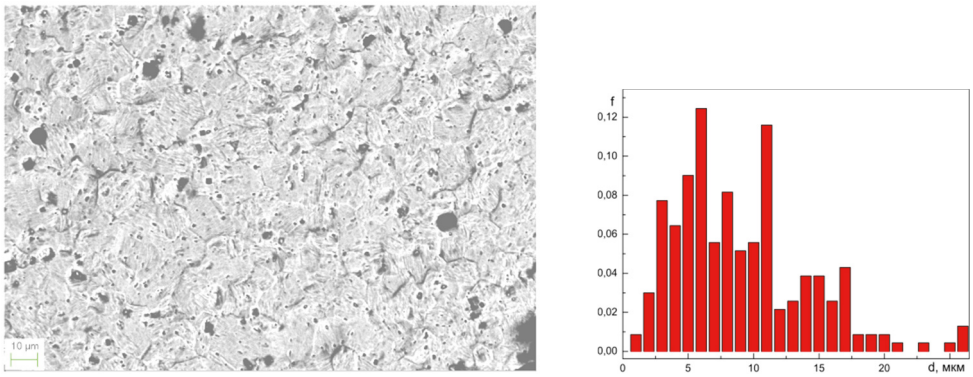

Fig. 2. Microstructure and grain size distribution of the CG $Ti_{49.1}Ni_{50.9}$ specimens.

When cooling and heating, the following sequence of martensitic transformation (MT) B2↔B19′ is realized in the CG specimens, and B2↔R↔B19′for UFG specimens. The MT temperatures in the wire specimens of the$Ti_{49.1}Ni_{50.9}$-alloy are shown in Table 1.

Table 1. Temperatures of martensitic transformation B2 ↔ R ↔ B19′ in specimens of the $Ti_{49.1}Ni_{50.9}$-alloy (at.%).

State	T_R, K	M_S, K	M_f, K	A_s, K	A_f, K
UFG	264	212	182	236	252
Recrystallization		241	221	252	263

Table 1 shows that both UFG and recrystallized specimens at 295K had the B2 phase structure before hydrogenation and prior to the beginning of isothermal loading when studying the development of inelastic and plastic deformations during torsion processes.

The stages of deformation development during isothermal (295K) loading when studying the UFG and recrystallized specimens are shown in Fig. 3. When reaching the martensitic shear stress (τ_M~410 MPa and ~350 MPa in UFG and recrystallized samples respectively), the stress–strain dependence of the samples exhibit typical features of B2 phase TiNi with the presence of a stress plateau, indicating the occurrence of stress-induced martensitic transformation (SIMT) and reorientation of the martensitic phases. This plateau passes into the stage of strain hardening, with the subsequent development of intensive plastic flow. Stress at the start of the last deformation stage decreases from 910 MPa in UFG specimens to 530 MPa in recrystallized specimens. Thus, transition from the UFG structure of specimens to the microcrystalline one, results in their softening. The simultaneous increase in MT temperatures leads to the decrease in τ_M, required for generation in the process of loading at 295K of the B19' martensite, providing the subsequent manifestation of superelasticity (SE) and shape memory effect (SME).

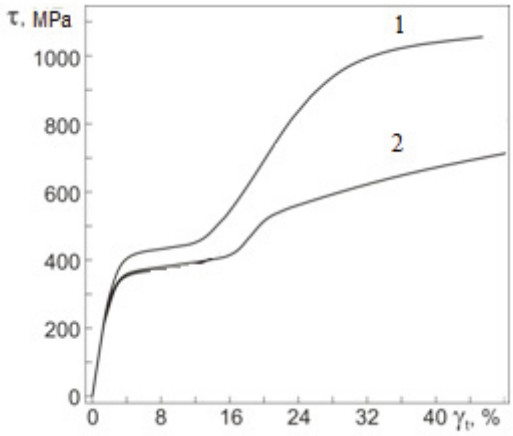

Fig. 3. Engineering “stress (τ)-strain (γ)” dependences during torsion of UFG specimens (1) and CG specimens (2) at T_{def} = 293 K

Before we proceed to the analysis of the hydrogen effect on the properties of the $Ti_{49.1}Ni_{50.9}$ alloy, let us consider how hydrogenation changes the hydrogen concentration in the studied specimens. The hydrogen content in the original specimens before hydrogenation was 7 wt. ppm. After electrochemical hydrogenation from the physiological solution of the specimens with UFG structure for 3 hours, the hydrogen content was about 400 wt. ppm. The measurements were performed after 1 or 2 hours after hydrogenation. It is considered that hydrogen can be easily released from TiNi due to the low activation energy of the hydrogen migration. According to the measurements performed in the hydrogenated specimens exposed for several days at room temperature, hydrogen content in the specimens remains almost at baseline. This is probably due to the rutile film forming on the surface of TiNi-alloy specimens and preventing hydrogen release.

The specimens with CG structure under the same hydrogenation conditions have shown much lower hydrogen content (175 wt. ppm.). This result is not surprising, since it is known that in fine crystalline metallic materials hydrogen is primarily concentrated at the grain boundaries. The hydrogen content in the UFG specimens should be higher due to the finer grain size and thus a more effective inner surface.

Since under these hydrogenation conditions, the hydrogen concentration exceeded a threshold concentration required for hydrogen embrittlement, in the next part of our study we compared the hydrogen effect on inelastic properties of the specimens with CG and UFG structure. Figures 4 and 5 present the results of tests on the inelastic strain accumulation and recovery under loading and unloading of the studied specimens at the first cycle before and after hydrogenation. Testing temperature was 296K. Figure 4 shows that in the CG specimens, the critical stress for austenitic-martensitic transformation, wherein a transition to the pseudoelastic plateau is observed, is approximately 360 MPa and the plateau length is about 12 per cent. The critical stress for austenitic-martensitic transformation in the specimens with SMC structure was approximately 70 MPa higher than in those with CG structure, Fig.5. After

unloading, the SMC specimens have lower residual strain (Fig.5), as compared to the CG specimens (Fig.4). After hydrogenation, a minor increase (by 10 MPa) in the critical stress of austenitic-martensitic transformation takes place in both parties of specimens. In literature it is connected with a solid solution strengthening due to the hydrogen atoms in interstitial positions. The hydrogenated CG specimens achieve the stage of "dislocation" strengthening earlier as compared to the unhydrogenated ones, Fig. 4.

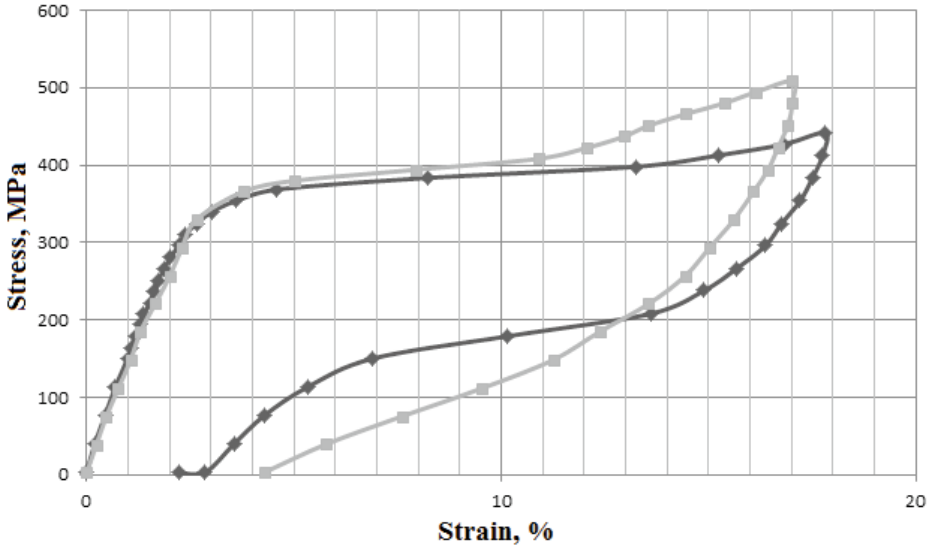

Fig. 4. Accumulation and recovery of the inelastic strain at the first "loading-unloading" cycle in the initial CG specimens of the $Ti_{49.1}Ni_{50.9}$ alloy before (♦) and after hydrogenation (▫). Testing temperature was 296 K.

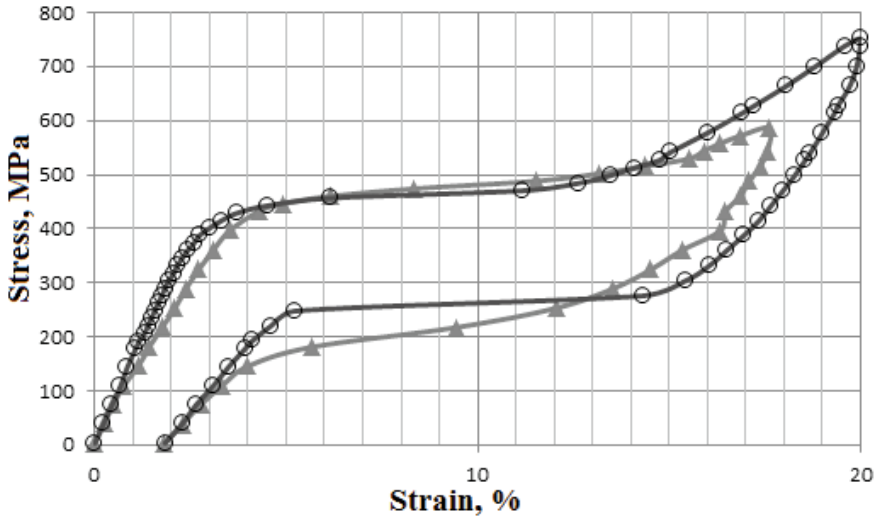

Fig. 5. Accumulation and recovery of the inelastic strain at the first "loading-unloading" cycle in the UFG specimens of the $Ti_{49.1}Ni_{50.9}$ alloy before (▲) and after hydrogenation (○). Testing temperature was 296 K.

Superelasticity of specimens of TiNi-based alloy after hydrogenation remains high (15 %) under external loading of less than 600 MPa.

Figure 6 presents the most significant changes revealed after the second loading cycle up to the failure of specimens, when the HE phenomenon appeared. It turned out that the hydrogenated specimens are subjected to substantially lower ultimate strain before the failure (21 per cent and 27 per cent, respectively in the specimen with CG and UFG structure) against approximately 50 per cent and 44 per cent in unhydrogenated specimens.

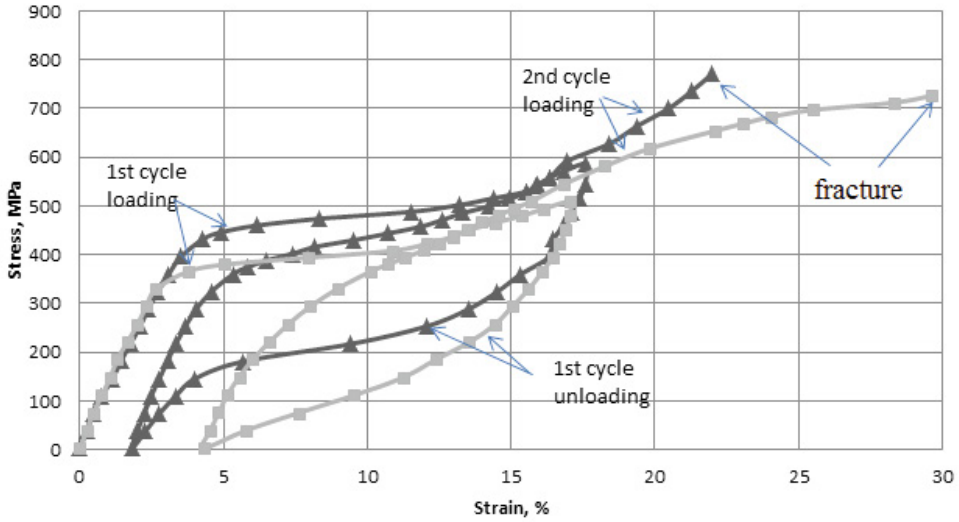

Fig. 6. Dependences of strain accumulation and recovery in first two "loading-unloading" cycles for the hydrogenated specimens with CG (▲) and UFG (■) structure. Testing temperature was 296 K.

Let us consider the regularities revealed under the fractographic study of fractured specimens after hydrogenation of the $Ti_{49.1}Ni_{50.9}$ alloy specimens. This paper presents only the research results of hydrogenated CG specimens. Previously, such studies have been conducted, for example, by Ogawa et al. (2015) but under the tensile strain. In this paper, the torsion strain is used. In paper by Miyabe et al. (2012) it is shown that a system of parallel circular cracks appears under tensile deformation of the hydrogenated cylindrical wire specimens on the surface of fractured specimens. The cracks appear in the hydrogenated thin and brittle layer. The distance between them is determined by the hydrogenated layer thickness that is dependent on the hydrogenation time. The similar regularities are also revealed in this paper. The scanning electron microscopy (SEM) was used to examine the surfaces of the fractured torsion specimens charged with 175 wt. ppm hydrogen. Figure 7 shows a system of parallel spiral cracks located on average at a distance of $\Delta l = 1.3$ mm apart that occurs under torsion strain. In contrast to Miyabe et al. (2012), in this case, cracks develop at an angle of 45 degrees in relation to the longitudinal axis of the wire. Along one of such cracks, the specimen fracture occurs, Fig.7. The specimen center shows a rather ductile fracture, unlike the near-surface layer, which fractures brittly.

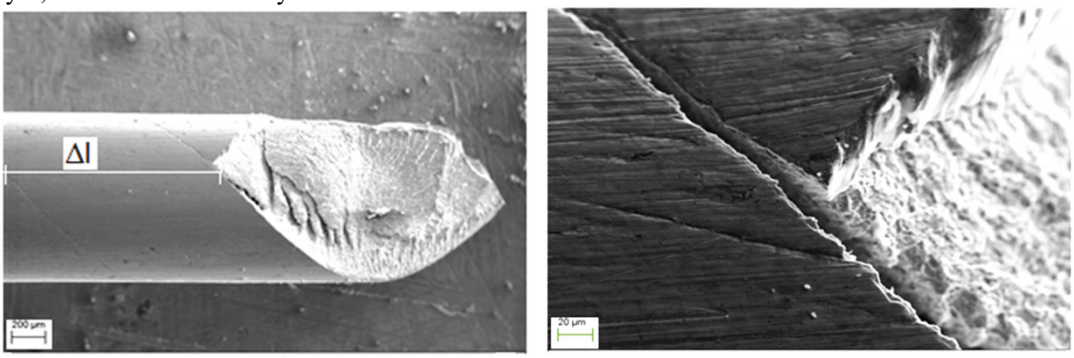

Fig. 7. SEM images of fracture surfaces of the hydrogenated TiNi specimens. Δl is the distance between spiral cracks on the wire surface.

This fracture pattern much differs from that, which is observed under torsion fracture of unhydrogenated TiNi specimens James et al. (2005). A distinctive feature of the torsion-fractured unhydrogenated specimens of the TiNi wire is a flat fracture surface, nearly perfectly orthogonal to the longitudinal axis of the wire.

Figures 7 and 8 show that cracks are opened after the fracture, and the extent of their opening decreases when removing from the specimen fracture plane.

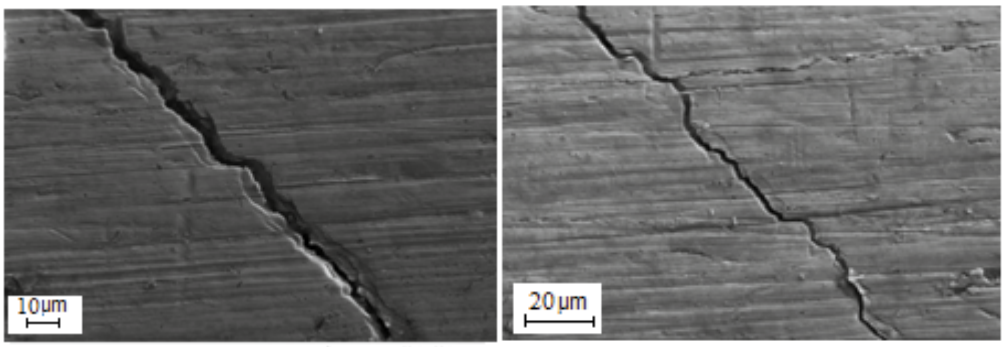

Fig. 8. Cracks on the surface of the fractured hydrogenated recrystallized specimens of the $Ti_{49.1}Ni_{50.9}$ alloy.

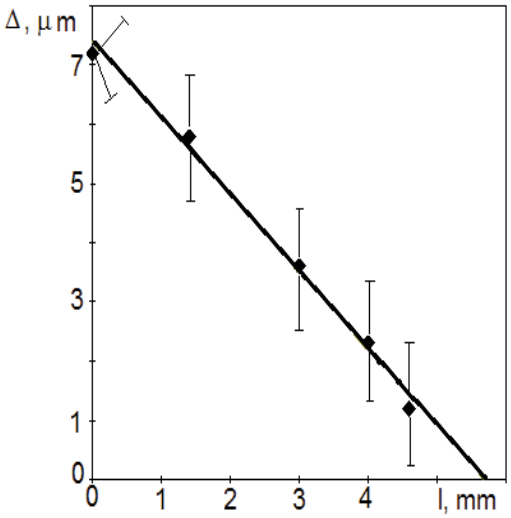

Fig. 9. The crack width dependence on distance specimen fracture plane.

The literature analysis has shown that the discovered regularities are observed when the brittle layer Panin et al. (2003) is formed on the plastic substrate. At the first stage of hydrogen saturation of Ti strength specimens increase simultaneously. This is due to the effect of the brittle surface layer. With increasing in the duration of hydrogen treatment strength and plasticity of Ti decrease owing to the hardened surface layer embrittlement.

For future work, other wires from $Ti_{49.1}Ni_{50.9}$ alloy with different aging time will be tested.

4. Conclusion

1. Wire specimens made of the$Ti_{49.1}Ni_{50.9}$ alloy with a UFG structure, absorb more than twofold hydrogen than those with CG structure.
2. Superelasticity of the alloy specimens after hydrogenation remains high under external loading of less than 600 MPa.
3. Hydrogen has a weaker effect on the inelastic properties of UFG specimens than on CG specimens.
4. The hydrogen embrittlement was found both in CG and in SMC specimens approximately at the same strain value, although at significantly different hydrogen content.

5. The SEM image of fracture surfaces of the hydrogenated specimens showed that increasing hydrogen content results in the brittle fracture mode.

Acknowledgements

The present work is financially supported by RFBR (project No. 15-08-99489) and partial financial support of Tomsk State University Competitiveness Improvement Program.

References

Asaoka, K., Yokoyama, K., Nagumo, M., 2002. Hydrogen embrittlement of nickel-titanium alloy in biological environment. Metallurgical and Materials Transactions A 33, 495-501.

Gamaoun, F., Hassine, T., 2014. Hydrogen effect on the austenite–martensite transformation of the cycled Ni-Ti alloy. Journal of Alloys and Compounds 615, 680-683.

Gamaoun, F., Ltaief, M., Bouraoui, T., Zineb, T., B., 2011. Effect of hydrogen on the tensile strength of aged Ni–Ti superelastic alloy Journal of Intelligent Material Systems and Structures 22, 2053–2059.

Ilin, A., A., Nazimov, O., P., Nikitich, A.,S., Chertov, S.,I., Gozenko, N., N., Skvortsova, S.,V., 1984. The effect of hydrogenation on structure and properties of the TN-1 alloy. Technology of light alloys 3, 42-47.

James, B., Foulds, J., Eiselstein, L., 2005. Failure analysis of NiTi wires used in medical applications. Journal of Failure Analysis and Prevention 5, 82-87.

Kireeva, I.,V., Chumlyakov, Yu.,I., Platonova, Yu., N., 2015. The effect of hydrogen on shape memory effect and superelasticity in single-phase nickel-titanium single crystals. Technical Physics Letters 41, 58-65.

Miyabe, N., Tanaka, H., Nakai, Y., Kawanishi T., 2012. Effect of hydrogen absorption on mechanical properties of TiNi shape memory alloy thin wire. Journal of the Society of Materials Science, Japan 61, 905-911.

Ogawa, T., Yokozawa, E., Oda, T., Maruoka, K., Sakai J. 2015. Hydrogen embrittlement behavior of Ni-Ti shape memory alloy with different microstructures in acidic fluoride solution. International Journal of Mechanical and Materials Engineering 10:12.

Panin, A.,V., Rybin, V.,V., Ushkov, S.,S., Kazachenok, M.,S., Klimenov, V., A., Pochivalov, Yu., I., Chernov, I., P., Tyurin, Yu., I., Nikitenkov, N., N., Lider A., M., Valiev, R., Z., 2003. Effect of hydrogen treatment on mechanical behavior of titanium with various structural states Physical Mesomechanics 6,17-24.

Pelton, B.,L., Slater, T., Pelton, A., R., 1997. Effect of hydrogen in TiNi, Proceeding 2nd International Conference on Shape Memory and Superelastic Technologies, Pacific Grove, CA, 395-400.

Yokoyama, K., Hamada, K., Moriama, K., Asaoka, K., 2001. Degradation and fracture of Ni-Ti superelastic wire in oral cavity. Biomaterials 32, 2257-2262.

Yokoyama, K., Nagaoka, A., Sakai, J., 2012. Effect of the hydrogen absorption conditions in the embrittlement behavior of Ni-Ti superelastic alloy. ISIJ International 52, 255-262.